ISBN: 978-3-95450-253-0 ISSN: 2673-5571 doi:10.18429/JACoW-HB2023-THBP24

RCS AND ACCUMULATOR RING DESIGNS FOR ISIS II

D. J. Adams, H. V. Cavanagh, B. Kyle, H. Rafique, C. M. Warsop, R. E. Williamson,
I. S. K. Gardner, ISIS Facility, STFC, Rutherford Appleton Laboratory, Oxfordshire, UK

Abstract

ISIS is the spallation neutron source at the Rutherford Appleton Laboratory in the UK, which provides 0.2 MW of beam power via a 50 Hz, 800 MeV proton RCS. Detailed studies are now underway to find the optimal configuration for a next generation, short-pulsed neutron source that will define a major ISIS upgrade, with construction beginning ~2031. Determining the optimal specification for such a facility is the subject of an ongoing study involving neutron users, target and instrument experts. The accelerator designs being considered for the MW beam powers required, include proposals exploiting FFA rings as well as conventional accumulator and RCS rings. This paper summarises work on physics designs for the conventional rings. Details of lattice designs, injection and extraction systems, correction systems as well as detailed 3D PIC simulations used to ensure 0.1% losses and low foil hits are presented. Designs for a 0.4 to 1.2 GeV RCS and 1.2 GeV AR are outlined. Work on the next stages of the study are also summarised to benchmark and minimise predicted losses, and thus maximise the high intensity limit of designs.

INTRODUCTION

The present working specification for the proposed ISIS II Facility requires $1.3\text{x}10^{14}$ protons per pulse (ppp) at 1.2 GeV and a repetition rate of 50 Hz. This 1.25 MW beam will supply multiple user targets to produce neutrons and muons for condensed matter research [1]. Consultation with the user communities and evaluation of accelerator technology, cost and sustainability are ongoing and may change the accelerator technologies and beam parameters.

The options outlined here are a 0.4 – 1.2 GeV Rapid Cycling Synchrotron (RCS) and a 1.2 GeV Accumulator Ring (AR) which represent conventional machine options delivering the high power, 1 μs pulse length proton beams required. Both can be positioned on the RAL site adjacent to, and run in parallel with, the existing facility. Options to site the accelerator within existing accelerator halls would require unacceptable interruptions to the experimental program.

Each machine option has its own challenges in meeting the physics specification. The RCS, at lower injection energy, has higher space charge effects whilst the AR, with thicker foils, has higher foil heating. To sustainably operate these high power beams it is necessary to limit total ring losses to ~0.1% to prevent machine damage and allow hands-on maintenance. Main parameters are summarised in Table 1.

Table 1: Summary of main RCS and AR parameters

Parameter	RCS	AR
Energy (GeV)	0.4 – 1.2	1.2
Intensity (ppp)	$1.3\text{x}10^{14}$	$1.3\text{x}10^{14}$
Repetition Rate (Hz)	50	50
Mean Power (MW)	1.25	1.25
Circumference (m)	282	282
No Super Periods	4	4
Magnet Excitation	Sinusoidal	DC
Dipole Fields (T), L (m)	0.42–0.84, 3	0.84, 3
Quad Max Field (T), L (m)	0.44, 0.5	0.43, 0.5
Betatron Tunes (Q_x, Q_y)	6.40, 6.32	6.40,6.32
Gamma Transition	5.21	5.21
Peak RF Volts (h=2, 4) (kV/turn)	300, 150	50, 28
RF Frequency (h=2)(MHz)	1.52 – 1.91	1.91
Acceptances: painted, collimated, aperture (π mm mr unnorm.) ($\Delta p/p$ ±0.01)	400, 600, 750	300, 350, 500
Carbon Foil μg/cm^2, eff. %	300, 99.4	500, 99.4
Injection Septum (T), L(m)	0.49, 2	0.27, 4.5
Inj. Dump, L (m), P (kW)	170, 2.6	790, 5.9

RING AND LATTICE DESIGN

The same lattice design is used for both the RCS and AR. It is similar in structure to the SNS lattice [2] but with additional drift lengths in the arcs to accommodate RF in the RCS. The ring has four super periods, a 282.3 m circumference, comprising of four-cell FODO achromatic arcs and two-cell reverse doublets for the straights. The straight is optically symmetric, hence a central waist with small (β_x, β_y) = (4.20, 6.99) m, chosen as the ring injection point, see Fig. 1. Drift lengths of 4.32 m in the arc sections and 7.29 m, 9.82 m in the straights provide ample room for RF, injection and extraction systems. The lattice transition gamma is 5.21, well above γ_{max}=2.27 at 1.2 GeV. The nominal working point is (Q_x, Q_y)=(6.40, 6.32). This gives reasonable space for incoherent tune spreads of up to −0.3 and avoids structural resonances. As established on the existing ISIS ring, a flexible working point is a very important feature in high-intensity operation. The addition of 4 trim quadrupoles in each straight provide working point control between 6.2 and 6.5 in both planes. Chromaticity correction is achieved using sextupoles in the arc sections. Lattice magnets have been sized to keep fields below 1 T, considered a limit for 50 Hz RCS ramping rates.

ISBN: 978-3-95450-253-0 ISSN: 2673-5571 doi:10.18429/JACoW-HB2023-THBP24

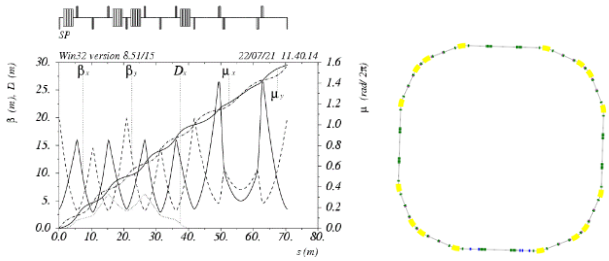

Figure 1: Lattice super period Twiss parameters, dispersion and phase advance (left) and ring layout (right).

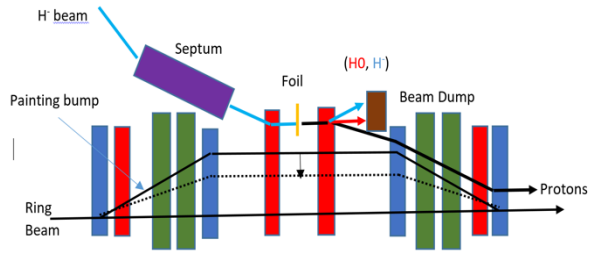

Figure 2: Schematic layout of injection straight: H, V painting bump magnets (blue), static bump magnets (red), and main ring quadrupoles (green).

BEAM DYNAMICS, APERTURES AND INSTABILITIES

As noted, the selected working point allows for $\Delta Q = -0.3$ without crossing systematic resonances. Detailed analysis of the lattice, and extensive 2D test runs with representative errors and expected space charge levels using ORBIT [3], indicate betatron resonances have minimal effects.

Acceptances are a key parameter for designs: making them too small results in unacceptable losses along with excessive foil re-circulations and temperatures, whilst making them larger increases magnet size and machine costs. Choices for acceptances here have been based on having the same space charge levels as those in the operational J-PARC machine [4], and the results of simulations described below. These lead to the 99% painted, collimated and full apertures shown in Table 1.

An initial assessment of possible longitudinal and transverse instabilities, based on the expected important resistive wall and space charge impedances, indicates transverse head-tail effects may be significant with chromaticity control a necessity. A more detailed impedance budget, along with suitable precautions including provision for damper systems and landau damping octupoles will be included in later stages of the design.

INJECTION AND ACCELERATION DESIGN

Injection designs use the H^- charge exchange process. For both the RCS and AR, injection is on the outside radius of the ring at the midpoint of a long straight, with the element arrangement shown in Fig. 2. Four static bump magnets displace the beam towards the injection point, the second of which is used to guide the incoming H^- beam from a septum onto the foil where 99.4% of the H^- beam is stripped to protons. Remaining partially or unstripped H^- and H^0, are guided through the third dipole onto a dump made from tungsten. Lorentz stripping of the H^- beam in the septum is a challenge to limit losses within a 1 W/m budget and requires a long low-field septum magnet. Beam is painted during injection using four additional magnets per plane which vary the ring closed orbit at the fixed injection point. Main parameters are given in Table 1.

Injection into the RCS is based on a 400 MeV linac supplying a 600 μs pulse length, 57.8 mA peak current H^- beam, which is chopped at ±60° of the h=2 ring RF for direct bucket injection. This beam is stripped to protons through a 300 μg/cm^2 carbon foil with 99.4% stripping efficiency accumulating 1.3x10^{14} protons over 455 turns in the ring. Transverse ring painting is correlated and oscillatory between 50 – 260 π mm mrad centroid emittances in both planes, Fig. 3. The oscillation in painting amplitudes achieves preferential beam distributions and reduced foil hits and has been optimised to avoid the $2Q_x - 2Q_y = 0$ coupling line and the integer line $Q_y = 6.0$. Attempts to reduce the overall painting further lead to incoherent tune spreads greater than 0.3 and excessive emittance growth. Longitudinal painting amplitudes of 0.3 to −1.8 MeV are achieved using RF bucket offsets with respect to the ring synchronous energy. This is timed symmetrically about field minimum of the sinusoidal main dipole field to minimise longitudinal painting offsets between the injection energy and ring synchronous energy. RF voltages are held constant over injection, at 77 kV, 40 kV per turn using a dual harmonic RF system with h=2 and h=4 cavities and peak at 300 kV, 150 kV during acceleration, Fig. 3.

For the AR case the injection energy is raised from 400 to 1200 MeV. Hence foil thickness increase to 500 μg/cm^2 to maintain 99.4% stripping efficiency and reduces the injection septum field from 0.49 T to 0.27 T to maintain Lorentz stripping losses < 1 W/m. Beam accumulation is now over 537 turns and centroid painting amplitudes are reduced to 21 – 174 π mm mrad due to lower space charge

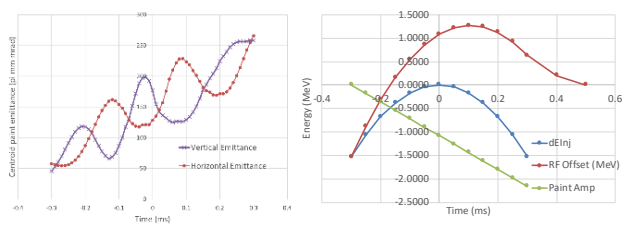

Figure 3: RCS transverse and longitudinal painting schemes.

ISBN: 978-3-95450-253-0 ISSN: 2673-5571 doi:10.18429/JACoW-HB2023-THBP24

effects. Longitudinal painting is constant at −3 MeV and beam is trapped using the same dual harmonic RF system with a constant voltage of 50 kV, 28 kV (h = 2, 4).

3D BEAM DYNAMICS

Detailed PIC simulations of injection with full 6D injection dynamics, space charge, magnet multipole errors and chromatic correction were undertaken with the code PyORBIT [5] for both the RCS and AR cases.

Higher space charge forces for the RCS case required careful optimisation of painting amplitudes to minimise maximum accumulated emittance, incoherent tune spreads and foil hits. Simulation studies at the end of injection, Fig. 4, show accumulated beam RMS emittances are ($\varepsilon_{x,rms}$, $\varepsilon_{y,rms}$)=(84.6, 71.2) π mm mrad and 99% occupancy emittances are ($\varepsilon_{x,99\%}$, $\varepsilon_{y,99\%}$)=(402.3, 369.1) π mm mrad. Probing the beam extremes with virtual scrapers shows the beam acceptance with 0.1% loss is 585 π mm mrad which is near expectations from space charge scaling of J-PARC i.e. 600 π mm mrad. Average foil hits were 2.26 per injected proton. Foil heating simulations show peak temperatures at the injection spot of 1652 K, well below the maximum 2000 K operating levels achieved at J-PARC.

For the AR case, lower space charge eased emittance optimisation. The accumulated beam RMS emittance were ($\varepsilon_{x,rms}$, $\varepsilon_{y,rms}$)=(44.9, 36.4) π mm mrad and 99% occupancy emittances ($\varepsilon_{x,99\%}$, $\varepsilon_{y,99\%}$)=(206.9, 180.4) π mm mrad. The 0.1% beam loss acceptance limit corresponded to 250 π mm mrad which is again near space charge scalings from J-PARC at 300 π mm mrad. Lower centroid painting amplitudes increased average foil hits to 3.46 per injected proton with corresponding foil peak temperatures of 1658 K, still well below 2000 K.

Acceleration simulations of the RCS case show a well-controlled longitudinal evolution but have continued transverse emittance growth which is the subject of further study.

CORRECTION, COLLIMATION AND EXTRACTION

Effects of ring magnet field and alignment errors were tested for many random distributions. These studies showed suitable quadrupole gradient corrections and steering magnet placements can easily be utilised to provide suitable correction of envelope and orbit errors.

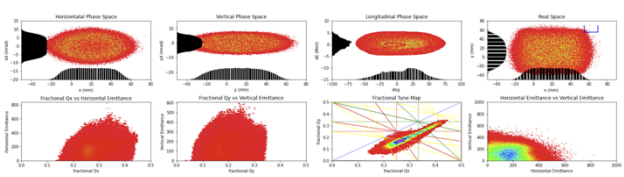

Figure 4: RCS beam parameter distributions clockwise from top left (x, x'), (y, y'), (ϕ, ΔE),(x, y), (ε_x, ε_y), (ΔQ_x, ΔQ_y), (ΔQ_y, ε_y), (ΔQ_x, ε_x) at injection end.

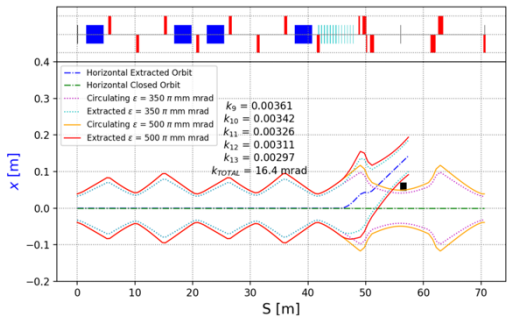

Figure 5: RCS extraction design.

Collimation designs in both the horizontal and vertical planes are based on two-stage primary and secondary systems placed in an achromatic straight section. Collimator acceptances are set at 650 π (RCS) and 350 π (AR) mm mrad, in both planes, with a phase advance separation of ~160° and are designed to intercept 0.1% of beam to protect the remainder of the ring to levels < 0.01%. Made from tungsten for superior stopping power, primary and secondary lengths are 1 mm and 200 mm for the RCS and 5 mm, 500 mm for the higher energy AR. In both cases the secondaries are stepped back ~3 – 5 mm to avoid the circulating proton beams. Momentum collimation design is underway with suitable placement in the dispersive arc. Studies of collimation placement using MADX [6] models show multiple solutions are possible for high capture efficiency. Further studies with full 6D PyORBIT are ongoing. Extraction is fast and single-turn, using kickers to horizontally deflect a beam into a septum around the centre region of a straight section, (β_x, β_y)=(4.20, 6.99) m. Technology is based on scaling existing ISIS kickers, 16 mrad deflection, 100 ns rise times, 1.5 m length at 800 MeV. New RCS extraction kicker requirements are, < 272 ns rise time, 19.9 mrad deflection to displace the beam at the septum entrance to 132.2 mm with corresponding parameters of < 182 ns, 16.4 mrad and 111.7 mm for the AR, Fig. 5. Given the increase in extraction energy from ISIS to ISIS II (0.8 – 1.2 GeV), the increased deflections require increasing lengths of the kicker magnets. New lengths of 2.71 m (RCS) and 2.24 m (AR) are easily placed in the super period short straight, 6.89 m.

CONCLUSIONS AND FURTHER STUDIES

Detailed, working physics designs of conventional AR and RCS rings for the ISIS II specification of 1.25 MW have been defined. More detailed studies of the 0.1% losses will ensure performance at or beyond present state of the art: this will involve more realistic magnet and impedance models with suitable experimental benchmarking. Future studies will also build in technology costs, reliability and sustainability requirements, including more detailed evaluation of full lifecycle carbon footprints.

ISBN: 978-3-95450-253-0 ISSN: 2673-5571 doi:10.18429/JACoW-HB2023-THBP24

REFERENCES

[1] "ISIS-II Design Summary Report", RAL, Oxford, UK, Rep. TN_ISIS2_008, 2022.

[2] S. Henderson *et al.*, "The Spallation Neutron Source accelerator system design'', *Nucl. Instrum. Methods Phys. Res., Sect. A* , vol. 763, pp. 610–673, 2014. doi:10.1016/j.nima.2014.03.067

[3] J. Galambos *et al*., "ORBIT - A ring injection code with space-charge", in *Proc. PAC'99*, New York, NY, USA, Mar. 1999, paper THP82, pp. 3143–3145.

[4] "Accelerator technical design report for high-intensity proton accelerator facility project", KEK, Tsukuba, Japan, Rep. KEK-2002-13. 2002.

[5] J.-F. Ostiguy and J. Holmes, "PyORBIT: A Python Shell for ORBIT", in *Proc. PAC'03*, Portland, OR, USA, May 2003, paper FPAG018, pp. 3503–3505.

[6] Mad-X website, http://madx.web.cern.ch/madx